Biophysical properties of membrane lipids of anammox bacteria

Boumann, Henry A.; Longo, Marjorie L.; Stroeve, Pieter; Poolman, Bert; Hopmans, Ellen C.; Stuart, Marc C. A.; Damste, Jaap S. Sinninghe; Schouten, Stefan

Published in:
Biochimica et Biophysica Acta-Biomembranes

DOI:
10.1016/j.bbamem.2009.04.008

Publication date:
2009

Biochimica et Biophysica Acta 1788 (2009) 1444–1451

Contents lists available at ScienceDirect

Biochimica et Biophysica Acta

journal homepage: www.elsevier.com/locate/bbamem

Biophysical properties of membrane lipids of anammox bacteria: I. Ladderane phospholipids form highly organized fluid membranes

Henry A. Boumann [a], Marjorie L. Longo [b], Pieter Stroeve [b], Bert Poolman [c], Ellen C. Hopmans [a], Marc C.A. Stuart [d], Jaap S. Sinninghe Damsté [a], Stefan Schouten [a,*]

[a] Department of Marine Organic Biogeochemistry, NIOZ Royal Netherlands Institute for Sea Research, PO Box 59, 1790 AB, Den Burg, Texel, The Netherlands
[b] Department of Chemical Engineering and Materials Science, University of California Davis, 1 Shields Ave, Davis, CA 95616, USA
[c] Department of Membrane Biochemistry, University of Groningen, Nijenborgh 4, 9747 AG, Groningen, The Netherlands
[d] Department of Biophysical Chemistry, University of Groningen, Nijenborgh 4, 9747 AG, Groningen, The Netherlands

ARTICLE INFO

Article history:
Received 9 November 2008
Received in revised form 2 April 2009
Accepted 8 April 2009
Available online 17 April 2009

Keywords:
Anammox bacteria
Ladderane phospholipid
Acyl chain ordering
Langmuir monolayer
Fluorescence depolarization
Micropipette aspiration

ABSTRACT

Anammox bacteria that are capable of anaerobically oxidizing ammonium (anammox) with nitrite to nitrogen gas produce unique membrane phospholipids that comprise hydrocarbon chains with three or five linearly condensed cyclobutane rings. To gain insight into the biophysical properties of these 'ladderane' lipids, we have isolated a ladderane phosphatidylcholine and a mixed ladderane phosphatidylethanolamine/phosphatidylglycerol lipid fraction and reconstituted these lipids in different membrane environments. Langmuir monolayer experiments demonstrated that the purified ladderane phospholipids form fluid films with a relatively high lipid packing density. Fluid-like behavior was also observed for ladderane lipids in bilayer systems as monitored by cryo-electron microscopy on large unilamellar vesicles (LUVs) and epi-fluorescence microscopy on giant unilamellar vesicles (GUVs). Analysis of the LUVs by fluorescence depolarization revealed a relatively high acyl chain ordering in the hydrophobic region of the ladderane phospholipids. Micropipette aspiration experiments were applied to study the mechanical properties of ladderane containing lipid bilayers and showed a relatively high apparent area compressibility modulus for ladderane containing GUVs, thereby confirming the fluid and acyl chain ordered characteristics of these lipids. The biophysical findings in this study support the previous postulation that dense membranes in anammox cells protect these microbes against the highly toxic and volatile anammox metabolites.

1. Introduction

Anammox bacteria play an essential role in the global marine nitrogen cycle and in waste waters as they are capable of anaerobically oxidizing ammonium (anammox) with nitrite into nitrogen gas [1–4]. This naturally occurring process is restricted to a distinct phylogenetic group of Brocadiales that is related to the *Planctomycetes* that currently holds the five genera *Candidatus* "Brocadia", *Candidatus* "Kuenenia", *Candidatus* "Anammoxoglobus", *Candidatus* Jettenia, and *Candidatus* "Scalindua" [3,5–7]. While the 16S rRNA gene sequence similarity of these genera is less than 85%, they possess similar morphological and physiological characteristics [6,8,9]. Their habitats include wastewater treatment systems, where anammox bacteria were originally discovered, as well as fresh water and oceanic systems [1,4,9,10].

A detailed study on the biochemical nature of the anammox process showed that nitrogen gas is produced from equimolar amounts of ammonium and nitrite [11]. While this conversion is the most important energy source for these lithotrophic organisms, it proceeds very slowly and cell proliferation takes place only once every 2–3 weeks [3]. A key enzyme mediating the anammox process is hydroxylamine/hydrazine oxidoreductase [12–14]. Both immuno-fluorescence microscopy and electron microscopy combined with immunogold labeling revealed that hydrazine oxidase is localized exclusively in a massive intracellular membrane compartment called the anammoxosome [15–18]. In *Candidatus* Brocadia spp., this organelle-like structure occupies more than 30% of its total cell volume [18]. It has been proposed that the anammoxosomal membrane is of vital importance for preserving an electrochemical proton gradient, which is required for ATP synthesis [18]. Moreover, the intracytoplasmic anammoxosome is also vital for cell viability as it

Abbreviations: 18:1–06:0 NBD-PC, 1-oleoyl-2-[6-[(7-nitro-2-1,3-benzoxadiazol-4-yl) amino]hexanoyl]-*sn*-glycero-3-phosphocholine; SOPS, 1-stearoyl-2-oleoyl-*sn*-glycero-3-phosphoserine; DPH, 1,6-diphenyl-1,3,5-hexatriene; DPPC, 1,2-dipalmitoyl-*sn*-glycero-3-phosphocholine; DSPC, 1,2-distearoyl-*sn*-glycero-3-phosphocholine; GC–MS, gas chromatography mass spectrometry; GUV, giant unilamellar vesicles; HPLC-ESI-MS/MS, high performance liquid chromatography electrospray ionization tandem mass spectrometry; LUV, large unilamellar vesicle; PC, phosphatidylcholine; PE, phosphatidylethanolamine; PG, phosphatidylglycerol; SOPC, 1-stearoyl-2-oleoyl-*sn*-glycero-3-phosphocholine; TLE, total lipid extract; TMA-DPH, 1-[4-(trimethylamino) phenyl]-6-phenylhexa 1,3,4-triene

* Corresponding author. Tel.: +31 222 369300; fax: +31 222 319674.
E-mail address: schouten@nioz.nl (S. Schouten).

0005-2736/$ – see front matter © 2009 Elsevier B.V. All rights reserved.
doi:10.1016/j.bbamem.2009.04.008

might protect the cell from the highly reactive anammox intermediates hydrazine, nitric oxide and/or hydroxylamine [19]. As these toxins likely can readily diffuse across membranes composed of conventional lipids, the anammoxosome must be comprised of specialized membrane building blocks to provide a dedicated permeability barrier.

Sinninghe Damsté and co-workers have investigated the membrane components of the anammoxosome by GC–MS and high field NMR, and revealed novel lipid structures that are unique in membrane biology. The membranes of anammox bacteria possess for the largest part lipids with alkyl chains possessing three or five cyclobutane rings tandemly fused by *cis*-ring junctions, designated

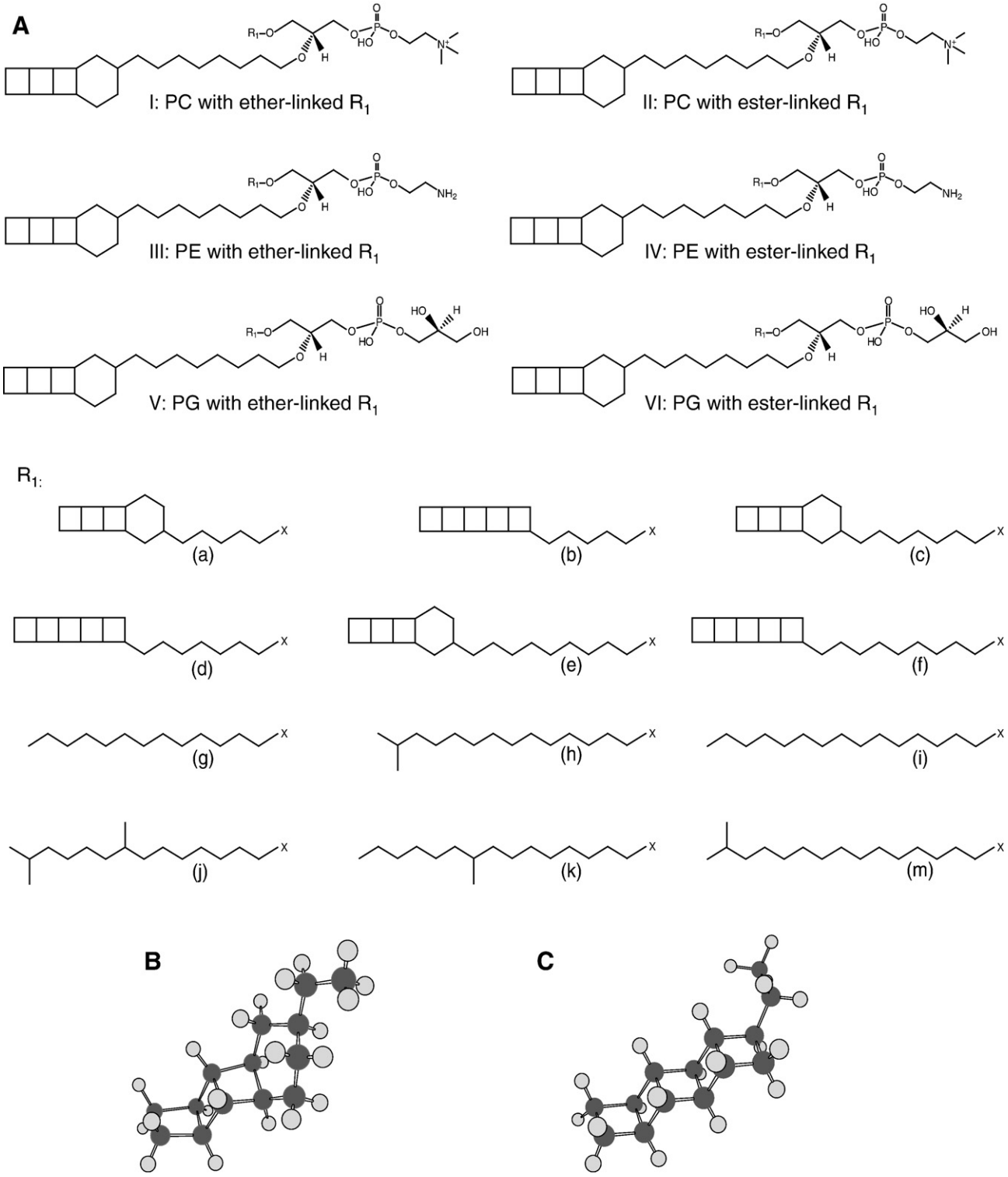

Fig. 1. Major phospholipids present in anammox bacteria. (A) The general structures of the PC, PE and PG diether lipids are shown by I, III and V, respectively. Structures II, IV and VI depict the ether–ester lipids of PC, PE and PG, respectively. The R_1 hydrocarbon chain (a–m) are: (a) C_{18}-[3]-ladderane, (b) C_{18}-[5]-ladderane, (c) C_{20}-[3]-ladderane, (d) C_{20}-[5]-ladderane, (e) C_{22}-[3]-ladderane, (f) C_{22}-[5]-ladderane, (g) pentadecane, (h) 14-methylpentadecane, (i) hexadecane, (j) 9,14-dimethylpentadecane, (k) 10-methylhexadecane, (m) 15-methylhexadecane, with X = COOH or CH_3OH. (B) and (C) show the three-dimensional illustration of the [3]- and [5]-ladderane structures, respectively [19].

[3]- and [5]-ladderanes, respectively, with the [3]-ladderanes being condensed to a cyclohexane ring (Fig. 1) [19–21]. The *sn*-2 position of the glycerol backbone of these lipids is typically occupied by an ether-linked C_{20}-[3]-ladderane moiety [21,22]. The hydrocarbon chains at *sn*-1 position are more structurally diverse and include a variety of ladderane, straight chain and methyl branched hydrocarbon chains that are either etherified or esterified to the glycerol backbone. The headgroups of these ladderane lipids comprise phosphocholine, phosphoethanolamine or phosphoglycerol moieties [23,24] (Fig. 1). Besides ladderane phospholipids, anammox membranes also comprise the cholesterol-like C_{35} bacteriohopanetetrol [23–25].

Although these extraordinary ladderane lipids have now been structurally well characterized, very little is known about their functional role in the cell. Previously, it was demonstrated that the diffusion of fluorophores across ladderane containing membranes was significantly lower than across conventional membranes [19]. Molecular modeling studies showed that a bilayer composed of a lipid with an etherified C_{20}-[3]-ladderane and an esterified C_{20}-[5]-ladderane hydrocarbon chain formed an exceptionally dense membrane [19].

In the present study, we isolated lipid fractions containing ladderane phosphatidylcholine (PC) and a mixture of ladderane phosphatidylethanolamine (PE) and ladderane phosphatidylglycerol (PG). We characterized these components in different membrane-like environments such as lipid monolayers and both large and giant unilamellar vesicles (LUVs and GUVs, respectively). The membrane fluidity and the acyl chain ordering of intact ladderane phospholipids have been studied using Langmuir monolayer and fluorescence depolarization experiments. Ladderane phospholipids were also examined by micropipette aspiration to elucidate their mechanical properties in GUVs. The results are discussed in the light of lipid packing of highly organized lipid membranes.

2. Materials and methods

2.1. Lipid material

About 5 L of a suspension of anammox biomass grown at 25 °C was collected from an oxygen limited wastewater treatment plant at Paques B.V. (Balk, The Netherlands). Fluorescence *in situ* hybridization analysis confirmed the dominance of *K. stuttgartiensis* in the reactor sample as described previously [23]. The suspension was lyophilized yielding ~40 g of dried biomass and the total lipid extract was isolated using a modified Bligh–Dyer procedure [26]. A solvent mixture of phosphate buffer/methanol/dichloromethane 0.8/2.0/1.0 (*v*/*v*/*v*) was added to the biomass. After 10 min of ultrasonication, dichloromethane and phosphate buffer were added to a volume ratio of 0.9/1.0/1.0 (*v*/*v*/*v*), followed by centrifuging to collect the dichloromethane fraction. The residual substance was re-extracted twice using the same procedure and the lipids were harvested from the dichloromethane fraction by rotary evaporation.

For control experiments, 1,2-distearoyl-*sn*-glycero-3-phosphocholine (DSPC), 1-stearoyl-2-oleoyl-*sn*-glycero-3-phosphocholine (SOPC) and 1,2-dipalmitoyl-*sn*-glycero-3-phosphocholine (DPPC) were purchased from Avanti Polar Lipids (Alabaster, AL).

2.2. Analysis of ladderane lipids

For compositional analysis, aliquots of the anammox total lipid extract were dissolved in dichloromethane/methanol ratios 9:1 (*v*/*v*) at 1.0 mg mL^{-1} and subjected to high performance liquid chromatography electrospray ionization tandem mass spectrometry (HPLC-ESI-MS/MS). For this purpose, an Agilent 1100 series LC (Agilent, San Jose, CA) was used and coupled to a Thermo TSQ Quantum ultra EM triple quadruple mass spectrometer with an Ion Max source equipped with an electrospray ionization probe (Thermo Electron Corporation, Waltham, MA) [23,24]. Liquid chromatography was accomplished on a Lichrospher column (250 mm × 2.1 mm, 5 mm particles; Alltech Associates Inc., Deerfield, IL) maintained at 30 °C. Two linear phase solutions were used: mixture A with hexane/2-propanol/formic acid/14.8 M NH_3 ratios 79/20/0.12/0.04 (*v*/*v*/*v*/*v*) and mixture B with 2-propanol/water/formic acid/14.8 M NH_3 ratios 88/10/0.12/0.04 (*v*/*v*/*v*/*v*). The applied flow rate was 0.2 mL min^{-1}, starting with 90% A to 35% A over 45 min, maintained for 20 min, then back flushed to 100% A for 20 min. Lipids were monitored by a data dependent MS routine in positive ion mode. First, a mass scan (*m*/*z* 300–1000) was performed. Subsequently, the base peak of the generated mass spectrum was fragmented in a MS/MS experiment [collision energy 20 V, collision gas (argon) 0.8 m Torr]. The $[M+H]^+$ ions of PC lipids were monitored by parental ion scanning for *m*/*z* 184, whereas the $[M+H]^+$ ions of PE and the $[M+NH_4]^+$ ions of PG were detected by neutral loss scanning for their characteristic fragments of 141 and 189 Da, respectively.

2.3. Isolation of ladderane phospholipids

Selected phospholipid classes of ladderane lipids were isolated by repeated semi-preparative HPLC using an HP 1100 LC system (Hewlett Packard, Palo Alto, CA) equipped with a thermostatted autoinjector and a column oven coupled to an Isco Foxy Jr. Fraction collector (Lincoln, NE). After injection of the filtered lipid extract onto a LiChrospher DIOL 100 Å (250 × 10 mm, 5 μm; Alltech) column, all fractions were eluted using the identical gradient and mobile phase composition described above for the HPLC-ESI-MS/MS analysis, but with a flow rate of 3 mL min^{-1}. The eluate was collected in 1 min fractions and small aliquots were analyzed by flow injection analysis using the same HPLC system as described above, coupled to an HP 1100 MSD mass spectrometer equipped with ESI source [27]. Fractions containing ladderane PC diether and/or PC ether–ester lipids were pooled and dried by rotary evaporation, yielding a lipid mixture that was designated 'PC ladderane fraction'. The fractions containing the co-eluting ladderane PE and PG diether and ether–ester lipids were also collected and pooled. The latter is referred to as the 'PE/PG ladderane fraction'. To remove residual ionic compounds like ammonium formate, both fractions were re-extracted as described above. Subsequently, the purities of all ladderane lipid containing samples were determined by weighing the samples and calculating the inorganic phosphorus contents on the basis of colorimetric measuring [28].

2.4. Langmuir monolayers

Surface pressure-mean area per molecule isotherms were obtained using a Teflon® Langmuir–Blodgett trough with dimensions 20 cm by 30 cm (Type 611, Nima, Coventry, United Kingdom). Lipids were dissolved in chloroform at 1.0 mg mL^{-1}. About 75 μL of a given lipid solution was gently released onto the water subphase at room temperature (23 ± 1 °C) using a 100 μL Hamilton microsyringe (Hamilton, Reno, NV). The barrier speed of the instrument was set at 20 cm^2 min^{-1} while the surface pressure of the film was measured using a Wilhelmy plate made of filter paper. Each surface pressure–area curve was recorded at least three times. Langmuir data was analyzed by determining the isothermal compressibility, k_s, as shown in Eq. (1), where *A* and π represent the molecular occupied area and film pressure, respectively:

$$\kappa_s = -\frac{1}{A}\frac{dA}{d\pi} \quad (1)$$

Furthermore, we used the MS data (Fig. 2) to estimate the mean molecular weights of 775 and 750 g mol^{-1} for the PC and PE/PG ladderane mixtures, respectively.

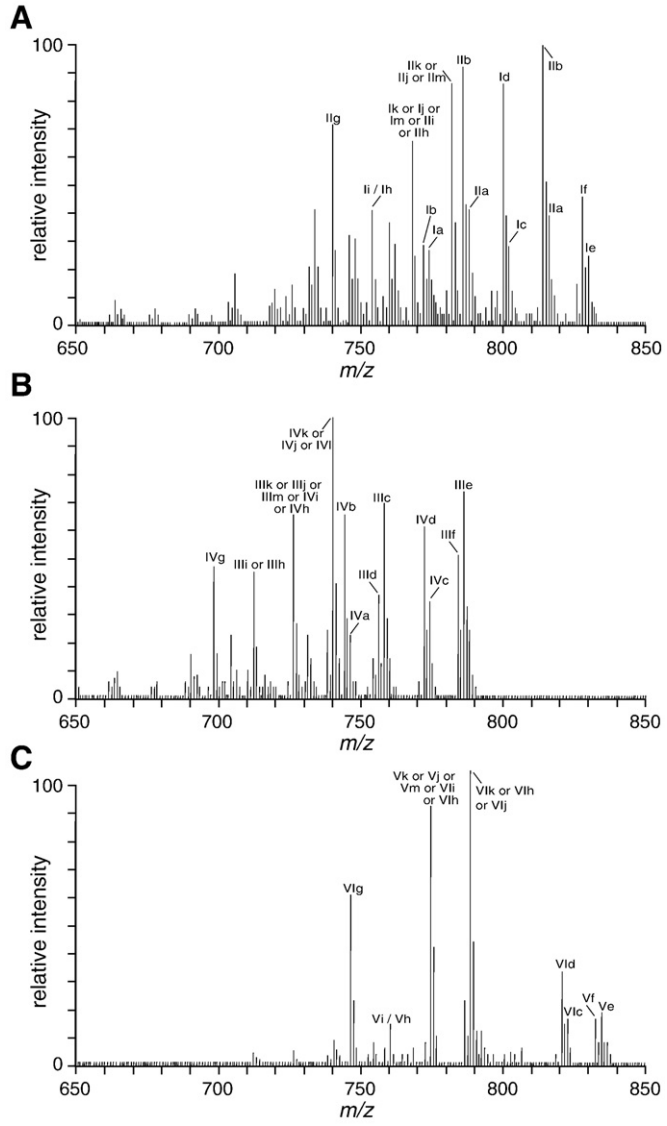

Fig. 2. Mass spectrometry analysis of the purified ladderane fractions. (A) ESI-MS/MS analysis of PC species in the isolated PC ladderane fraction by parent ion scanning for m/z 184. (B) ESI-MS/MS spectrum of the PE lipids in the isolated PE/PG ladderane fraction obtained by neutral loss scanning for m/z 141. (C) Molecular species profile of PG in the PE/PG ladderane fraction monitored by neutral loss scanning for m/z 189. For peak denotation, see Fig. 1.

2.5. Cryo-electron microscopy of large unilamellar vesicles

LUVs at a lipid concentration of 50 μM were prepared by hydrating a lyophilized lipid film in 50 mM potassium phosphate (KP_i) buffer at pH 7.0. For that reason, five consecutive steps of freezing in liquid nitrogen and thawing at room temperature were followed by extrusion through a 200 nm polycarbonate filter. Cryo-electron microscopy was performed for the PC and PE/PG ladderane fractions according to standard procedures reported earlier [29]. A small droplet of liposome suspension was applied onto a glow-discharged holey carbon-coated grid (Quantifoil 3.5/1) and excessive fluid was removed using filter paper. Grids were vitrified in liquid ethane. Specimens were monitored using a Philips CM 120 cryo-electron microscope (Eindhoven, The Netherlands) operating at 120 kV and equipped with a Gatan cryo-holder (model 626, Gatan, Pleasanton, CA). Micrographs were recorded under low-dose conditions with a Gatan (model 794MSC) slow CCD camera.

2.6. Fluorescence microscopy of giant unilamellar vesicles

GUVs were prepared by electroformation as described previously [30–32]. Here, we generated GUVs using PC ladderane lipids with 1 mol% of 1-oleoyl-2-[6-[(7-nitro-2-1,3-benzoxadiazol-4-yl)amino] hexanoyl]-*sn*-glycero-3-phosphocholine (18:1–06:0 NBD-PC) (Avanti Polar Lipids). GUV imaging was performed with Nikon Eclipse 400 fluorescence microscope (Nikon, Melville NY) equipped with a fluorescence filter cube (EF-4 FITC HYQ, Nikon).

2.7. Fluorescence depolarization

Fluorescence depolarization experiments were conducted for the anammox and *E. coli* total lipid extracts, using a Fluorolog®-3 Instrument (Horiba Jobin Yvon, Edison, NJ), according to Shinitzky and Barenholz [33]. For experiments using 1,6-diphenyl-1,3,5-hexatriene (DPH) (Invitrogen, Eugene, OR), lipids were dried by rotary evaporation and hydrated in 50 mM KP_i buffer, pH 7.0 to produce liposomes as described above. LUVs at a lipid concentration of 50 μM in 50 mM KP_i buffer, pH 7.0 were incubated in the presence of $5.0 \cdot 10^{-8}$ M DPH. Excitation and emission wavelength were set at 360 nm and 428 nm, respectively. For the 1-[4-(trimethylamino)phenyl]-6-phenylhexa 1,3,4-triene (TMA-DPH) (Invitrogen) labeling of liposomes, 5 μL TMA-DPH stock solution (4 mM in dimethylsulfoxide) was diluted into 245 μL 50 mM KP_i buffer, pH 7.0. Subsequently, the liposomes were mixed with TMA-DPH solution in a 1:1 volume ratio, resulting in a TMA-DPH/lipid ratio of 1:125 (mol/mol). After incubation for 1 h at room temperature, the steady state fluorescence depolarization was measured upon a 40-fold dilution of the liposomes. The excitation and emission wavelength were recorded at 360 nm and 430 nm, respectively. All experiments were performed using a Lauda Model RE 106 temperature controlled water bath (Lauda-Königshofen, Germany).

2.8. Micropipette aspiration of giant unilamellar vesicles

Mechanical properties of GUVs were studied by video microscopy of micropipette aspiration as described in detail by Longo and Ly [32]. For this purpose, GUVs were prepared as described above, with the exception of adding 0.5 mol% of 1-stearoyl-2-oleoyl-*sn*-glycero-3-phosphoserine (SOPS) instead of 1.0 mol% 18:1–06:0 NBD-PC to prevent vesicle fusion. Micropipettes with an inner diameter tip of 6 to 8 nm were used after coating with SurfaSil® (Pierce, Rockford, IL). The micropipettes were filled with 100 mM glucose containing 0.02% total wt. bovine serum albumin solution to diminish vesicle adhesion to the glass surface. The position of the micropipette was controlled with a micromanipulator (model MHW-3, Narishige, Japan). Clean GUVs were gently pre-stressed and the aspiration pressure was varied to gradually increase the membrane tension. Alterations in the projection length of the vesicle were recorded on video [32]. We used a Nikon microscope equipped with a 403 Hoffman modulation contrast objective (Modulation Optics, Greenvale, NY), a high-resolution charge-coupled device camera (Dage MTI, Michigan City, IN), a manometer slider with linear encoder (Velmex, Bloomfield, NY) and a video overlay box (Polvision, Western Australia). The suction pressure, ΔP, applied to a vesicle was determined from the change in height of a water manometer coupled to the micropipette. The membrane tension, τ, was calculated using Eq. (2), and depends on the suction pressure and the geometry of both the vesicle and micropipette [32,34].

$$\tau = \frac{\Delta P R_p}{2\left(1 - \frac{R_p}{R_v}\right)} \tag{2}$$

The vesicle radius, R_v, and change in length of projection, ΔL, were measured by video imaging and converted into microns through

calibration with a known grid. The radius of the pipette, R_p, was measured by inserting a probe with a known length–diameter relationship, as determined from electron microscopy, into the micropipette. The change in surface area (A–A_0), normalized by the initial area A_0 equals the area strain, α. The area strain was determined from the projection length using the approximate relationship shown in Eq. (3) [32].

$$\alpha = \frac{2\pi R_p \Delta L}{A_0}\left(1 - \frac{R_p}{R_v}\right) \quad (3)$$

Area compressibility measurements were conducted by gradually increasing the suction pressure and by determining the change in the projection length. The apparent area compressibility modulus, K_A, was obtained from the linear slope of the tension *versus* area strain in the high-tension regime, given that $\tau > 0.5$ mN/m. Similar rates of suction pressure increase were applied during repeated measurements. All experiments were conducted at room temperature.

3. Results and discussion

3.1. Isolation of ladderane phospholipids

Since an axenic culture of anammox bacteria is still lacking to date, we have obtained a total lipid extract from an enrichment (about 75% purity) culture of anammox bacteria derived from a wastewater treatment plant in Balk, the Netherlands. In agreement with previous detailed HPLC-MS/MS and GC–MS characterization studies, most components of the total lipid extract were PC, PE and PG lipids that possess at least one ladderane hydrocarbon chain (see Fig. 1 and [21–24]).

For the study of biophysical properties of ladderane lipids it would be desirable to obtain individual ladderane phospholipid species in high purity. Unfortunately, the chromatographic separation of these lipids is mainly determined by polarity of their headgroup moiety rather than the nature of the hydrocarbons [23,24,35]. Furthermore, due to the large molecular diversity in ladderane lipids, it would have been difficult to obtain purified material in sufficient quantities. We therefore isolated a fraction containing only PC diethers/ether–ester ladderane lipids and a fraction containing the PE and PG diethers/ether–ester ladderane lipids (purities about 85%). Fig. 2 depicts the ESI-MS/MS spectra for the isolated PC- and PE/PG ladderane fractions. These profiles showed that they exclusively consist of phospholipids with one or two ladderane hydrocarbon chains.

3.2. Packing of ladderane phospholipid monolayers

We performed Langmuir monolayer experiments at room temperature (23 ± 1 °C) to obtain information on the biophysical behavior of ladderane lipids, using DSPC and SOPC as references. After the lift-off, the solid phase DSPC monolayer exhibited an onset pressure increase near 56 Å^2/molecule and collapsed at a pressure of ~62 mN/m (Fig. 3A, black diamonds). For SOPC, the isotherm showed an initial pressure increase at approximately 105 Å^2/molecule and further increasing of the surface pressure destabilized the liquid-expanded phase lipid film near 47 mN/m (Fig. 3A, white diamonds). Extrapolation of the slope of the isotherm of DSPC to zero pressure revealed a minimal packing density of ~54 Å^2 per molecule, whereas SOPC showed a minimal packing of 85 Å^2 per lipid molecule. These findings are in good agreement with the literature and illustrate that the presence of one double bond in a straight hydrocarbon chain of a lipid already affects the packing of phospholipids in monolayers [36–38].

Fig. 3B depicts the isotherms obtained for the PC- and PE/PG ladderane fractions. The monolayers of the PC- and PE/PG ladderane lipids exhibited a first pressure increase at about 76 and 67 Å^2 per mean molecule, respectively. For an accurate assessment of physical

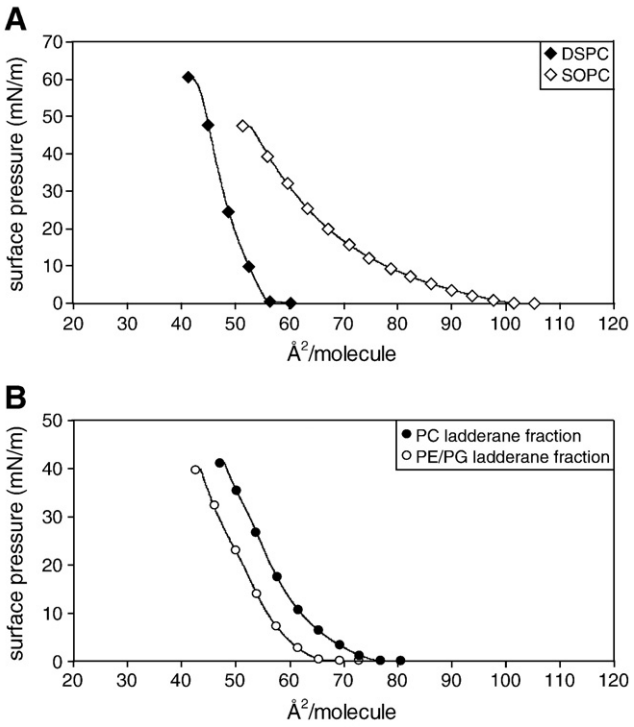

Fig. 3. Surface pressure–area per molecule isotherms of (A) DSPC (black diamonds) and SOPC (white diamonds) and (B) the PC ladderane fraction (black circles) and the PE/PG ladderane fraction (white circles). All experiments were performed at least three times at room temperature.

state of the Langmuir films, we determined the isothermal surface compressibility values and obtained at the same pressures, a comparable k_s value for the SOPC and ladderane monolayers, but a much lower k_s value for DSPC. For example, at 30 mN/m, the k_s values for SOPC, PC- and PE/PG ladderane lipids were about 0.010 m/mN, whereas the k_s value of DSPC was 0.0035 m/mN. Thus, both ladderane containing monolayers remained in the liquid-expanded phase at elevated surface pressure and collapsed at ~41 mN/m. This indicates that the ladderane lipids formed fluid lipid films regardless of their relatively high lipid ordering. The average minimal area per molecule for the PC- and the PE/PG ladderane lipids were near 65 and 59 Å^2/molecule, respectively, hence close to the minimal packing density of DSPC. As the ladderane mixtures were mainly composed of phospholipids with C_{18}-[3]-, C_{18}-[5]-, C_{20}-[3]- and C_{20}-[5]-ladderane hydrocarbon chains, these experiments support the hypothesis that ladderane lipids are capable of forming relatively dense membranes [19].

3.3. Formation of large and giant unilamellar vesicles

The proposed dense and fluid ladderane lipid architecture was further investigated in a lipid bilayer environment using LUVs. Imaging of these vesicles by cryo-electron-microscopy showed that both PC- and PE/PG ladderane containing LUVs were spherically shaped at room temperature, hence characteristic for vesicles comprising fluid-phase lipids (Fig. 4A and B, *cf.* [29]). We estimated that the ladderane liposomes exhibit a membrane thickness near 4 nm, which is similar to that of membranes comprised of DPPC [39]. A ChemProMM2 calculation of one of the most abundant PC ladderane lipid (Fig. 1B) in minimal energy configuration suggest a length of ~2.4 nm for this lipid and thus a bilayer composed of this membrane would have a thickness of maximally ~4.8 nm. The slightly lower observed bilayer thickness suggests there may be some interdigitation of the ladderane phospholipids bilayers.

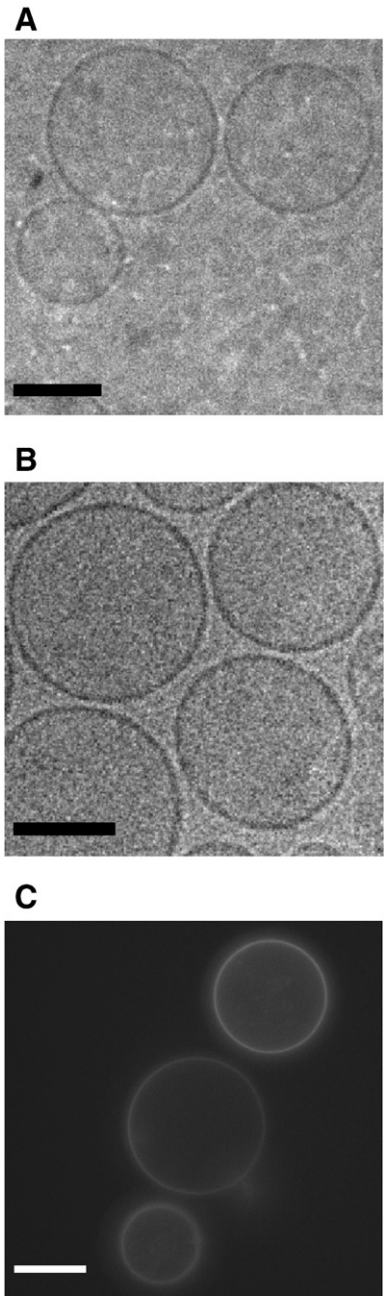

Fig. 4. Microscopy analysis of ladderane lipid vesicles. Cryo-electron images of LUVs composed of (A) the PC ladderane fraction and (B) the PE/PG ladderane fraction. The scale bars indicate 100 nm. (C) GUVs composed of PC ladderane lipids labeled with 1 mol% of 18:1–06:0 NBD-PC showing a homogenous fluorescence corresponding to a single fluid phase, at least on the macromolecular scale probed by light microscopy. The scale bar represents 25 μm.

GUVs are useful model systems of biological membranes to investigate lipid domain formation and phase behavior at macroscopic scales, as well as membrane deformation processes and mobility of membrane components [31,40,41]. Fig. 4C shows a typical confocal image of GUVs composed of the isolated PC ladderane lipid mixture labeled with 18:1–06:0-NBD-PC at room temperature. Since the probe preferentially co-localizes with fluid-phase lipids, the homogeneous fluorescence intensity distribution of the spherical PC ladderane GUVs points toward the existence of a single fluid phase [42]. We obtained similar images when the PC ladderane GUVs were cooled down to 4 °C, thereby confirming the miscibility of this mixture of fluid-like phospholipids (data not shown). In addition, the membrane contour was always smooth and spherical, typical of a fluid phase, whereas in contrast a gel-phase often gives facetted contours [43]. While no GUVs could be prepared from the PE/PG ladderane mixture, the PC ladderane fraction typically yielded a large population of GUVs ranging from 20 to 100 μm in diameter.

3.4. Acyl chain ordering in ladderane phospholipids

The acyl chain ordering of the ladderane lipid containing membranes was examined by using the fluorescent membrane-embedded probes DPH and TMA-DPH [33,44,45]. Fig. 5A shows the fluorescence intensities for DPH which preferentially anchors within the interior of the hydrophobic region of bilayers of LUVs [46]. The reference DPPC LUVs showed DPH fluorescence depolarization intensities higher than 0.44 at temperatures below its phase transition at 42 °C (Fig. 5A, grey circles). In agreement with earlier studies, lower fluorescence depolarization intensities were observed at elevated temperatures due to more rotational freedom of the probe [47–49].

For the PC ladderane fraction, the temperature dependent DPH fluorescence depolarization profile was significantly different (Fig. 5A, black circles). In the absence of a phase transition, the DPH fluorescence intensity almost linearly decreased from about 0.40 to 0.14. At room temperature, the DPH fluorescence intensity of the PC ladderane fraction was close to 0.26, indicating fluid-like membranes

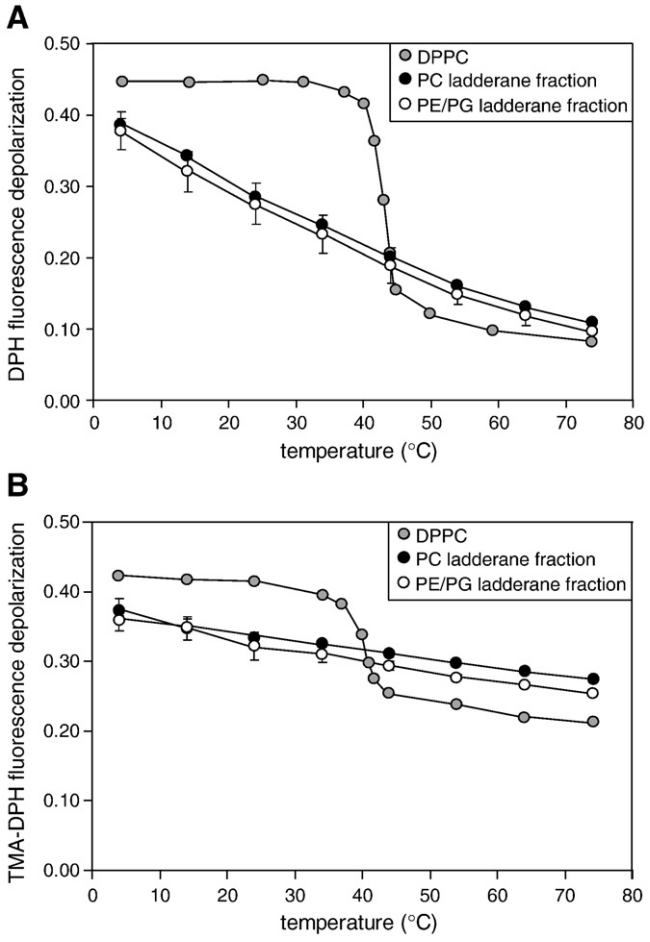

Fig. 5. (A) Fluorescence depolarization of DPH in membrane vesicles prepared from DPPC (gray circles), the PC ladderane fraction (black circles) and the PE/PG ladderane fraction (white circles). (B) Fluorescence depolarization of TMA-DPH in membrane vesicles from DPPC (gray circles), the PC ladderane fraction (black circles) and the PE/PG ladderane fraction (white circles). The data points of the latter two represent the mean values ± the standard deviation of three independent experiments.

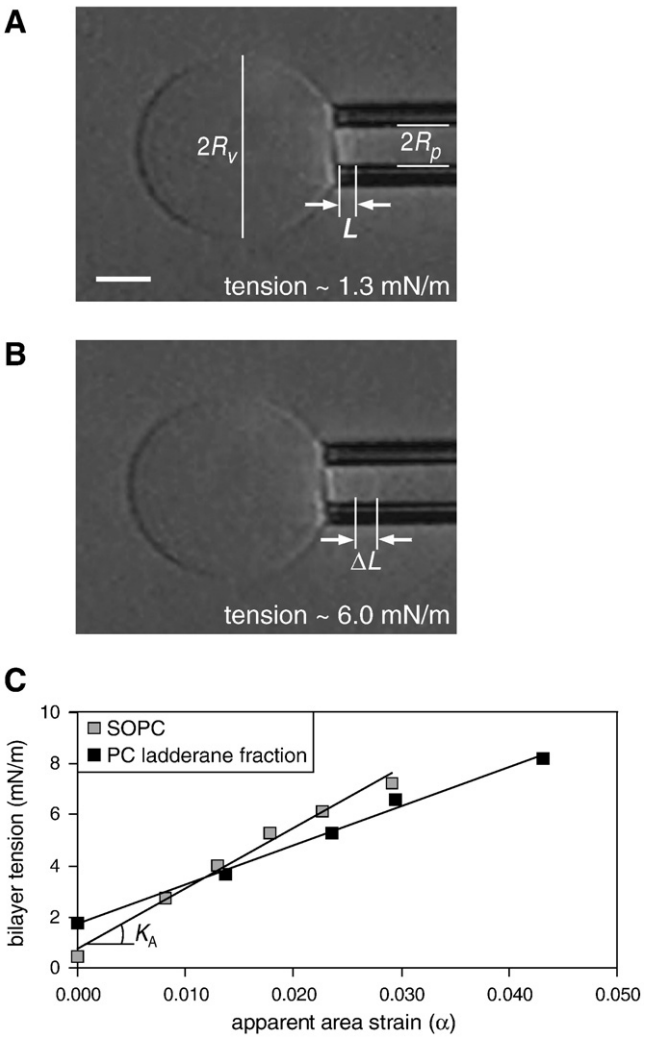

Fig. 6. Mechanical properties of GUVs determined by micropipette aspiration. Video micrographs of a PC ladderane vesicle aspired inside a micropipette in a glucose solution. An increase, ΔL, in the projection length, L, is observed when the applied membrane tension, τ, was changed from (A) a low tension of 1.3 mN/m, to (B) a high tension of 6.0 mN/m. The vesicle radius, R_v, and the radius of the pipette, R_p, are also indicated. The scale bar represents 10 nm (C) Averaged tension *versus* strain measurements for GUVs composed of SOPC (gray squares) and PC ladderane lipids (black squares). The area compressibility, K_A, was determined by fitting the tension as a function of apparent area strain.

with a relatively high acyl chain ordering. A similar trend was observed for the DPH depolarization profile of the PE/PG ladderane fraction (Fig. 5A, white circles). Hence, the relatively more acyl chain ordering and fluid nature of the ladderane containing LUVs lipids support the Langmuir monolayer data, which show isotherms with high slopes, *i.e.* a high elastic modulus and thus more acyl chain ordering and viscosity (Fig. 3B).

The results for the TMA-DPH depolarization experiments are shown in Fig. 5B. In contrast to DPH, TMA-DPH senses the lipid packing at the periphery of the hydrophobic core of the lipid bilayer [46]. We measured a moderate decline in the TMA-DPH depolarization intensities for DPPC near the phase transition temperature, consistent with previous studies (Fig. 5B, gray circles, [49,50]). For the isolated PC- and PE/PG ladderane fractions, we observed only minor gradual changes in the temperature dependency of TMA-DPH depolarization, indicating that that acyl chain ordering is most pronounced in the interior of the membrane where the cyclobutane ring structures are located (Figs. 1B, C and 5B).

3.5. Mechanical properties of ladderane vesicles

The influence of the ladderane hydrocarbon chains on the mechanical properties in lipid bilayers was examined by micropipette aspiration. By applying suction pressure to GUVs using a manometer coupled micropipette, we could monitor changes in projected area of the vesicle with changes in membrane tension (see Materials and methods, [32,34,51,52]). Fig. 6A and B depict video micrographs of a PC ladderane assembled GUV at different suction tensions. As a reference, we monitored SOPC GUVs since these vesicles exhibit bilayers with fluidity and thickness characteristics comparable to the lipid fraction of biological membranes [34]. Consistent with previous findings, we observed a K_A of 154 ± 18 dyn cm^{-1} for SOPC (Fig. 6C, gray squares, [52,53]). The measurements for PC ladderane lipids revealed a K_A of 191 ± 72 dyn cm^{-1}, thus showing a stiffer, but still fluid, behavior compared to the SOPC GUVs (Fig. 6C, gray squares). For comparison, previous studies have shown that approximately 30% cholesterol is required to increase K_A in SOPC GUVs to that of the PC ladderane GUVs [34]. We suggest that the large standard variation for the K_A value for the PC ladderane lipids might be due to compositional fluctuations of the different GUVs formed from the PC ladderane lipid fraction. It is worth mentioning that these fluctuations could not be detected by epi-fluorescence microscopy. Nevertheless, these findings are in line with the above biophysical experiments and show that the ladderane containing GUVs are in a fluid state but have more acyl chain ordering than membranes composed of lipids with conventional hydrocarbon chains.

4. Conclusions

The present study shows for the first time that mixtures containing solely lipids with ladderane hydrocarbon chains can be used to constitute both monolayers and liposomes. Despite their closely packed and relatively rigid nature, these lipid systems also convey a fluid-like behavior. These findings support the hypothesis that ladderane lipids may form membranes that are essential for protecting anammox cells against highly toxic metabolic intermediates like hydrazine and for preventing proton leakage from the anammoxosome organelle [19].

Acknowledgements

The authors would like to thank Dr. J. M. Kuiper for technical assistance with fluorescence depolarization measurements. Paques BV (Balk, the Netherlands) is gratefully acknowledged for providing anammox cell material. Drs Marc Strous and Mike Jetten are thanked for fruitful discussions. This work was financially supported by the 'From Molecule to Cell Program' of the Netherlands Organization for Scientific Research (NWO) and granted to S.S. and J.S.S.D (805.47.097). NanoNed and the Zernike Institute obtained additional support for Advanced Materials (to BP).

References

[1] M.C. Schmid, N. Risgaard-Petersen, J. van de Vossenberg, M.M. Kuypers, G. Lavik, J. Petersen, S. Hulth, B. Thamdrup, D. Canfield, T. Dalsgaard, S. Rysgaard, M.K. Sejr, M. Strous, H.J. den Camp, M.S. Jetten, Anaerobic ammonium-oxidizing bacteria in marine environments: widespread occurrence but low diversity, Environ. Microbiol. 9 (2007) 1476–1484.
[2] M.M. Kuypers, G. Lavik, D. Woebken, M. Schmid, B.M. Fuchs, R. Amann, B.B. Jorgensen, M.S. Jetten, Massive nitrogen loss from the Benguela upwelling system through anaerobic ammonium oxidation, Proc. Natl. Acad. Sci. U. S. A. 102 (2005) 6478–6483.
[3] M. Strous, J.A. Fuerst, E.H. Kramer, S. Logemann, G. Muyzer, K.T. van de Pas-Schoonen, R. Webb, J.G. Kuenen, M.S. Jetten, Missing lithotroph identified as new planctomycete, Nature 400 (1999) 446–449.
[4] T. Dalsgaard, D.E. Canfield, J. Petersen, B. Thamdrup, J. Acuna-Gonzalez, N2 production by the anammox reaction in the anoxic water column of Golfo Dulce, Costa Rica, Nature 422 (2003) 606–608.

[5] Z.X. Quan, S.K. Rhee, J.E. Zuo, Y. Yang, J.W. Bae, J.R. Park, S.T. Lee, Y.H. Park, Diversity of ammonium-oxidizing bacteria in a granular sludge anaerobic ammonium-oxidizing (anammox) reactor, Environ. Microbiol 10 (2008) 3130–3139.
[6] B. Kartal, J. Rattray, L.A. van Niftrik, J. van de Vossenberg, M.C. Schmid, R.I. Webb, S. Schouten, J.A. Fuerst, J.S. Damste, M.S. Jetten, M. Strous, Candidatus "*Anammoxoglobus propionicus*" a new propionate oxidizing species of anaerobic ammonium oxidizing bacteria, Syst. Appl. Microbiol. 30 (2007) 39–49.
[7] M. Schmid, K. Walsh, R. Webb, W.I. Rijpstra, K. van de Pas-Schoonen, M.J. Verbruggen, T. Hill, B. Moffett, J. Fuerst, S. Schouten, J.S. Damste, J. Harris, P. Shaw, M. Jetten, M. Strous, Candidatus "*Scalindua brodae*", sp. nov., Candidatus "*Scalindua wagneri*", sp. nov., two new species of anaerobic ammonium oxidizing bacteria, Syst. Appl. Microbiol. 26 (2003) 529–538.
[8] J. van de Vossenberg, J.E. Rattray, W. Geerts, B. Kartal, L. van Niftrik, E.G. van Donselaar, J.S. Sinninghe Damste, M. Strous, M.S. Jetten, Enrichment and characterization of marine anammox bacteria associated with global nitrogen gas production, Environ. Microbiol 10 (2008) 3120–3129.
[9] M.S. Jetten, O. Sliekers, M. Kuypers, T. Dalsgaard, L. van Niftrik, I. Cirpus, K. van de Pas-Schoonen, G. Lavik, B. Thamdrup, D. Le Paslier, H.J. Op den Camp, S. Hulth, L.P. Nielsen, W. Abma, K. Third, P. Engstrom, J.G. Kuenen, B.B. Jorgensen, D.E. Canfield, J.S. Sinninghe Damsté, N.P. Revsbech, J. Fuerst, J. Weissenbach, M. Wagner, I. Schmidt, M. Schmid, M. Strous, Anaerobic ammonium oxidation by marine and freshwater planctomycete-like bacteria, Appl. Microbiol. Biotechnol. 63 (2003) 107–114.
[10] M.M. Kuypers, A.O. Sliekers, G. Lavik, M. Schmid, B.B. Jorgensen, J.G. Kuenen, J.S. Sinninghe Damsté, M. Strous, M.S. Jetten, Anaerobic ammonium oxidation by anammox bacteria in the Black Sea, Nature 422 (2003) 608–611.
[11] A.A. van de Graaf, A. Mulder, P. de Bruijn, M.S. Jetten, L.A. Robertson, J.G. Kuenen, Anaerobic oxidation of ammonium is a biologically mediated process, Appl. Environ. Microbiol. 61 (1995) 1246–1251.
[12] J. Schalk, S. de Vries, J.G. Kuenen, M.S. Jetten, Involvement of a novel hydroxylamine oxidoreductase in anaerobic ammonium oxidation, Biochemistry 39 (2000) 5405–5412.
[13] M. Shimamura, T. Nishiyama, K. Shinya, Y. Kawahara, K. Furukawa, T. Fujii, Another multiheme protein, hydroxylamine oxidoreductase, abundantly produced in an anammox bacterium besides the hydrazine-oxidizing enzyme, J. Biosci. Bioeng. 105 (2008) 243–248.
[14] M. Shimamura, T. Nishiyama, H. Shigetomo, T. Toyomoto, Y. Kawahara, K. Furukawa, T. Fujii, Isolation of a multiheme protein with features of a hydrazine-oxidizing enzyme from an anaerobic ammonium-oxidizing enrichment culture, Appl. Environ. Microbiol. 73 (2007) 1065–1072.
[15] M.R. Lindsay, R.I. Webb, M. Strous, M.S. Jetten, M.K. Butler, R.J. Forde, J.A. Fuerst, Cell compartmentalisation in planctomycetes: novel types of structural organisation for the bacterial cell, Arch. Microbiol. 175 (2001) 413–429.
[16] L. van Niftrik, W.J. Geerts, E.G. van Donselaar, B.M. Humbel, R.I. Webb, J.A. Fuerst, A.J. Verkleij, M.S. Jetten, M. Strous, Linking ultrastructure and function in four genera of anaerobic ammonium-oxidizing bacteria: cell plan, glycogen storage, and localization of cytochrome C proteins, J. Bacteriol. 190 (2008) 708–717.
[17] L. van Niftrik, W.J. Geerts, E.G. van Donselaar, B.M. Humbel, A. Yakushevska, A.J. Verkleij, M.S. Jetten, M. Strous, Combined structural and chemical analysis of the anammoxosome: a membrane-bounded intracytoplasmic compartment in anammox bacteria, J. Struct. Biol. 161 (2008) 401–410.
[18] L.A. van Niftrik, J.A. Fuerst, J.S. Sinninghe Damsté, J.G. Kuenen, M.S. Jetten, M. Strous, The anammoxosome: an intracytoplasmic compartment in anammox bacteria, FEMS Microbiol. Lett. 233 (2004) 7–13.
[19] J.S. Sinninghe Damsté, M. Strous, W.I. Rijpstra, E.C. Hopmans, J.A. Geenevasen, A.C. van Duin, L.A. van Niftrik, M.S. Jetten, Linearly concatenated cyclobutane lipids form a dense bacterial membrane, Nature 419 (2002) 708–712.
[20] M.A. Miller, J.M. Schulman, AM1, MNDO and MM2 studies of concatenated cyclobutanes: prismanes, ladderanes and asteranes, J. Mol. Struct. 163 (1988) 133–141.
[21] J.S. Sinninghe Damsté, W.I. Rijpstra, J.A. Geenevasen, M. Strous, M.S. Jetten, Structural identification of ladderane and other membrane lipids of planctomycetes capable of anaerobic ammonium oxidation (anammox), FEBS J. 272 (2005) 4270–4283.
[22] J.S. Sinninghe Damsté, W.I. Rijpstra, M. Strous, M.S.M. Jetten, O.R.P. David, J.A.J. Geenevasen, J.H. van Maarseveen, A mixed ladderane/n-alkyl glycerol diether membrane lipid in an anaerobic ammonium-oxidizing bacterium, Chem. Commun (2004) 2590–2591.
[23] H.A. Boumann, E.C. Hopmans, I. van de Leemput, H.J. Op den Camp, J. van de Vossenberg, M. Strous, M.S. Jetten, J.S. Sinninghe Damste, S. Schouten, Ladderane phospholipids in anammox bacteria comprise phosphocholine and phosphoethanolamine headgroups, FEMS Microbiol. Lett. 258 (2006) 297–304.
[24] J.E. Rattray, J. van de Vossenberg, E.C. Hopmans, B. Kartal, L. van Niftrik, W.I. Rijpstra, M. Strous, M.S. Jetten, S. Schouten, J.S. Damste, Ladderane lipid distribution in four genera of anammox bacteria, Arch. Microbiol 190 (2008) 51–66.
[25] J.S. Sinninghe Damsté, W.I. Rijpstra, S. Schouten, J.A. Fuerst, M.S.M. Jetten, M. Strous, The occurrence of hopanoids in planctomycetes: implications for the sedimentary biomarker record, Org. Geochem. 35 (2004) 561–566.
[26] E.G. Bligh, W.J. Dyer, A rapid method of total lipid extraction and purification, Can. J. Biochem. Physiol. 37 (1959) 911–917.
[27] R.H. Smittenberg, E.C. Hopmans, S. Schouten, J.S. Sinninghe Damste, Rapid isolation of biomarkers for compound specific radiocarbon dating using high-performance liquid chromatography and flow injection analysis-atmospheric pressure chemical ionisation mass spectrometry, J. Chromatogr. A 978 (2002) 129–140.
[28] C.H. Fiske, Y. Subbarow, The colorimetric determination of phosphorus, J. Biol. Chem. 66 (1925) 375–400.
[29] M.C. Stuart, E.J. Boekema, Two distinct mechanisms of vesicle-to-micelle and micelle-to-vesicle transition are mediated by the packing parameter of phospholipid-detergent systems, Biochim. Biophys. Acta 1768 (2007) 2681–2689.
[30] M.K. Doeven, J.H. Folgering, V. Krasnikov, E.R. Geertsma, G. van den Bogaart, B. Poolman, Distribution, lateral mobility and function of membrane proteins incorporated into giant unilamellar vesicles, Biophys. J. 88 (2005) 1134–1142.
[31] N. Kahya, D. Scherfeld, K. Bacia, B. Poolman, P. Schwille, Probing lipid mobility of raft-exhibiting model membranes by fluorescence correlation spectroscopy, J. Biol. Chem. 278 (2003) 28109–28115.
[32] M.L. Longo, H.V. Ly, Micropipet aspiration for measuring elastic properties of lipid bilayers, Methods Mol. Biol. 400 (2007) 421–437.
[33] M. Shinitzky, Y. Barenholz, Fluidity parameters of lipid regions determined by fluorescence polarization, Biochim. Biophys. Acta 515 (1978) 367–394.
[34] D. Needham, R.S. Nunn, Elastic deformation and failure of lipid bilayer membranes containing cholesterol, Biophys. J. 58 (1990) 997–1009.
[35] H.F. Sturt, R.E. Summons, K. Smith, M. Elvert, K.U. Hinrichs, Intact polar membrane lipids in prokaryotes and sediments deciphered by high-performance liquid chromatography/electrospray ionization multistage mass spectrometry—new biomarkers for biogeochemistry and microbial ecology, Rapid Commun. Mass Spectrom. 18 (2004) 617–628.
[36] R.A. Demel, L.L.M. Van Deenen, B.A. Pethica, Monolayer interactions of phospholipids and cholesterol, Biochim. Biophys. Acta 135 (1967) 11–19.
[37] P. Dynarowicz-Latka, K. Hac-Wydro, Interactions between phosphatidylcholines and cholesterol in monolayers at the air/water interface, Colloids Surf., B: Biointerfaces 37 (2004) 21–25.
[38] M.C. Phillips, D. Chapman, Monolayer characteristics of saturated 1,2,-diacyl phosphatidylcholines (lecithins) and phosphatidylethanolamines at the air–water interface, Biochim. Biophys. Acta 163 (1968) 301–313.
[39] J.F. Nagle, S. Tristram-Nagle, Structure of lipid bilayers, Biochim. Biophys. Acta 1469 (2000) 159–195.
[40] F.S. Ariola, D.J. Mudaliar, R.P. Walvick, A.A. Heikal, Dynamics imaging of lipid phases and lipid-marker interactions in model biomembranes, Phys. Chem. Chem. Phys. 8 (2006) 4517–4529.
[41] S.A. Sanchez, L.A. Bagatolli, E. Gratton, T.L. Hazlett, A two-photon view of an enzyme at work: *Crotalus atrox* venom PLA2 interaction with single-lipid and mixed-lipid giant unilamellar vesicles, Biophys. J. 82 (2002) 2232–2243.
[42] W.C. Lin, C.D. Blanchette, T.V. Ratto, M.L. Longo, Lipid asymmetry in DLPC/DSPC-supported lipid bilayers: a combined AFM and fluorescence microscopy study, Biophys. J. 90 (2006) 228–237.
[43] K.J. Tierney, D.E. Block, M.L. Longo, Elasticity and phase behavior of DPPC membrane modulated by cholesterol, ergosterol, and ethanol, Biophys. J. 89 (2005) 2481–2493.
[44] B.R. Lentz, Use of fluorescent probes to monitor molecular order and motions within liposome bilayers, Chem. Phys. Lipids 64 (1993) 99–116.
[45] J.R. Hazel, Thermal adaptation in biological membranes: is homeoviscous adaptation the explanation? Annu. Rev. Physiol. 57 (1995) 19–42.
[46] R.D. Kaiser, E. London, Location of diphenylhexatriene (DPH) and its derivatives within membranes: comparison of different fluorescence quenching analyses of membrane depth, Biochemistry 37 (1998) 8180–8190.
[47] J.R. Wetterau, A. Jonas, Effect of dipalmitoylphosphatidylcholine vesicle curvature on the reaction with human apolipoprotein A-I, J. Biol. Chem. 257 (1982) 10961–10966.
[48] I. Konopasek, J. Vecer, K. Strzalka, E. Amler, Short-lived fluorescence component of DPH reports on lipid–water interface of biological membranes, Chem. Phys. Lipids 130 (2004) 135–144.
[49] F. Reig, I. Haro, D. Polo, M.A. Egea, M.A. Alsina, Interfacial interactions of hydrophobic peptides with lipid bilayers, J. Colloid Interface Sci. 246 (2002) 60–69.
[50] S. Shrivastava, A. Chattopadhyay, Influence of cholesterol and ergosterol on membrane dynamics using different fluorescent reporter probes, Biochem. Biophys. Res. Commun. 356 (2007) 705–710.
[51] W. Rawicz, K.C. Olbrich, T. McIntosh, D. Needham, E. Evans, Effect of chain length and unsaturation on elasticity of lipid bilayers, Biophys. J. 79 (2000) 328–339.
[52] H.V. Ly, M.L. Longo, The influence of short-chain alcohols on interfacial tension, mechanical properties, area/molecule, and permeability of fluid lipid bilayers, Biophys. J. 87 (2004) 1013–1033.
[53] S. Nichols-Smith, S.Y. Teh, T.L. Kuhl, Thermodynamic and mechanical properties of model mitochondrial membranes, Biochim. Biophys. Acta 1663 (2004) 82–88.